ELSEVIER

J. Non-Newtonian Fluid Mech. 86 (1999) 89–104

Journal of Non-Newtonian Fluid Mechanics

The effect of processing parameters on glass fiber birefringence development and relaxation

X. Lu, E.M. Arruda, W.W. Schultz*

Mechanical Engineering and Applied Mechanics, The University of Michigan, Ann Arbor, MI 48109-2125, USA

Received 30 May 1998; received in revised form 16 September 1998

Abstract

Birefringence of oxide glass fibers drawn from glass melts through an orifice has been detected previously [H. Stockhorst, R. Brückner, J. Non-Cryst. Solids 49 (1982) 471; H. Stockhorst, R. Brückner, J. Non-Cryst. Solids, 86 (1985) 105.] This birefringence is a measure of anisotropy in glass structure that can influence fiber performance properties. Birefringence is produced during fiber drawing as the fiber is rapidly stretched in the viscoelastic glass transition range. The birefringence is 'frozen' into the glass during rapid cooling. With a simple drawing apparatus using Borosilicate glass (Corning code 7740) preforms, we produce glass fibers for a range of process conditions and measure their as-drawn birefringence. The development of birefringence in glass fibers is found to depend on the amount of deformation, the deformation rate, and temperature. Results for various process parameters show that increasing draw ratio, increasing elongation rate, and decreasing draw temperature increase birefringence. Post-process annealing is used to examine the time and temperature dependent glass fiber birefringence relaxation. Birefringence is found to completely relax in the temperature range close to the glass transition range as expected, but it is also noted that birefringence shows substantial (although incomplete) relaxation in a temperature range well below the glass transition. This low temperature relaxation indicates that the relaxation process may be due to a distribution of relaxation times. A modified stretched exponential and a pair of Jeffrey elements in parallel are used to describe this distribution and capture birefringence relaxation in a wide range of temperatures below the glass transition range.

Keywords: Glass fibers; Birefringence; Nonisothermal; Relaxation

1. Introduction

It is well known that fibers have mechanical and physical properties that are substantially different from those of materials in their bulk forms. For instance, filaments usually have higher tensile strengths and stiffnesses [3–5]. We have demonstrated a strong correlation between birefringence and tensile strength during annealing [6]. The optical properties and molecular structures of the fibers and the bulk also differ. Process parameters and post-processing operations change the properties of fibers in a

* Corresponding author.

0377-0257/99/$ – see front matter
PII: S0377-0257(98)00203-1

manner that is thought to be related to the microstructure, but the relationship between various process parameters and fiber properties is not well understood. Birefringence in drawn glass fibers is a manifestation of structural anisotropy. In optical glass fibers drawn from preforms, birefringence is a well documented result of residual deformation caused by the different coefficients of thermal expansion of the cladding and core glasses [7]. Birefringence of drawn oxide glass fibers from orifices has been detected by Stockhorst and Brücker [1,2]. Less work has been done on the measurement of birefringence of oxide glass fibers drawn from preforms.

Birefringence of glass fibers is expected to be affected by fiber drawing process parameters such as drawing temperature, drawing speed, and the draw ratio – parameters that also affect fiber mechanical properties. Control and optimization of the drawing parameters and post processing treatment are essential to obtaining optimal optical and mechanical response in glass fibers. An understanding of the development of birefringence during glass fiber drawing and its relaxation during annealing can aid in assessing mechanical property enhancement in fiber drawing. Although the birefringence is small compared to that in polymers, there is relatively small data scatter as compared to the scatter in strength tests. Birefringence is a direct measure of anisotropy and should decay to zero for quasi-equilibrium (as opposed to calorimetry or measurements of density, index of refraction, etc.).

In this paper, we examine the effect of the drawing parameters such as drawing temperature, drawing and feed speed, and draw ratio on birefringence of fibers drawn from preforms. The use of preforms, while common in optical fiber drawing, is used here for simplifying the apparatus and to allow for a well described stress–strain temperature history (we found no measurable birefringence in any of our preforms). We also investigate the relaxation of birefringence during fiber annealing. Glass fiber birefringence is the optical manifestation of anisotropic structure that relaxes in a time and temperature dependent manner. Our experiments show that this relaxation near the glass transition range is similar to that of viscoelastic strain, however, at low temperature annealing, full fiber birefringence relaxation does not occur.

Structural relaxation is the process by which the material thermodynamic properties, such as enthalpy, volume and refractive index gradually approach their equilibrium value following changes in some external parameters, such as temperature and pressure. In general, structural relaxation is described by

$$\frac{P(T,t)-P(T,\infty)}{P(T,0)-P(T,\infty)}=M(T,t), \tag{1}$$

where $P(T, t)$ is any thermodynamic property of temperature (T) and time (t), $P(T, \infty)$ its equilibrium value, $P(T, 0)$ the initial value and $M(T, t)$ a relaxation function which for an isothermal process may have the form

$$M(T,t)=\exp(-t/\tau(T)) \tag{2}$$

For oxide glasses in the annealing range, fictive temperature (the temperature at which the present structure would be in equilibrium [8]) is commonly used to describe structural relaxation such that

$$\frac{\mathrm{d}T_\mathrm{f}}{\mathrm{d}t}=\frac{T-T_\mathrm{f}}{\tau}, \tag{3}$$

where the time constant τ has the linearized Arrhenius dependence on temperature and fictive

temperature as

$$\tau = \tau_0 \exp(-A_1 T - A_2 T_f), \tag{4}$$

where τ_0, A_1, and A_2 are constants. Tool's approach successfully captures the thermal expansion of annealed glass by using

$$M = \alpha_g (T - T_0) - \alpha (T_f - T_{f0}) \tag{5}$$

where α_g is the glassy state thermal expansion coefficient, T_0 a reference temperature, α a structure related coefficient, and T_{f0} the initial fictive temperature. This approach was unable to predict the thermal expansion data of the quenched glass under 500°C. Refractive index relaxation experiments by Ritland [9] have shown that a single fictive temperature evolution described by Eqs. (3) and (4) is not sufficient to describe the distributed nature of property relaxation. Since the as-drawn fiber is anisotropic, it is not in equilibrium for any temperature and only partial relaxation may occur, the use of a single fictive temperature to describe drawn fiber birefringence relaxation is questionable.

Narayanaswamy [10] proposed using a reduced time to compromise the temperature and fictive temperature effect. Linearity can be restored by using the reduced time parameter defined by

$$\xi = \tau(T_0) \int_0^t \frac{dt'}{\tau}, \tag{6}$$

where T_0 is an arbitrary reference temperature. Boltzmann's superposition principle describes T_f by

$$T_f = T - \int_0^\xi M(\xi - \xi') \frac{dT}{d\xi'} d\xi'. \tag{7}$$

The thermodynamic property $P(T, \xi)$ becomes

$$P(T, \xi) = P(T, \infty) - \alpha_s \int_0^\xi M(\xi - \xi') \frac{dT}{d\xi'} \, d\xi', \tag{8}$$

where $M(\xi - \xi')$ is a relaxation function most often described by a 'stretched exponential'

$$M(\xi) = \exp(-\xi/\tau)^b \tag{9}$$

for a constant b, and α_s is a structure parameter.

Based on the general Arrhenius relation $\tau_0 = \tau_0 \exp(\Delta H/RT)$, to describe thermally activated relaxation, Narayanaswamy suggested that the contribution of fictive temperature to structural relaxation could be included by partitioning the relaxation time in the following empirical form:

$$\tau = \tau_0 \exp\left(\frac{x \Delta H}{RT} + \frac{(1 - x) \Delta H}{RT_f}\right), \tag{10}$$

where τ_0 is a constant, ΔH an activation energy, R the ideal gas constant, and x a constant between 0

and 1. Later investigators [11–13] used the Adams–Gibbs equation based on the suggestion that the flow of the structure involves the cooperative rearrangement of increasingly large number of molecules as temperature decreases. Thus, the relaxation time depends on the configurational entropy as

$$\tau = \tau_0 \exp\left(\frac{A}{T\,\Delta S(T_k,\, T_f)}\right) \tag{11}$$

where $\Delta S(T_k,\, T_f)$ is the configurational entropy with structure corresponding to T_f, the Kauzmann temperature T_k is defined by the vanishing of the equilibrium value of ΔS, and τ_0 and A are constants. The phenomenolgical models based on the T–N equations successfully describe relaxation of those isotropic parameters such as density, refractive index and enthalpy in bulk glass in the glass transition range. Recently, differential scanning calorimetry (DSC) experiments in oxide glass fibers by Huang and Gupta [14] demonstrate that the T–N model is inadequate for describing enthalpy relaxation of drawn glass fibers at temperatures well below the glass transition range. Relaxation well below the glass transition temperature has also been observed in oxide glass [15], metal glass [16], and polymers [17].

Since birefringence in glass fibers is the result of frozen anistropic elastic strain, its relaxation is expected to behave similarly to that of viscoelastic strain recovery of inorganic glasses. Our experiments demonstrate this behavior for birefringence relaxation near the glass transition temperature T_g. We explore the use of a relaxation spectrum to simulate the relaxation of glass fiber birefringence. Low temperature (sub-T_g) birefringence relaxes to a non-zero value, suggesting that part of the frozen elastic strain remains. Over a very broad temperature range, the process is not only nonlinear but also non-thermal rheologically simple, i.e. the form of the relaxation function changes with temperature. We have modified the stretched exponential function to simulate the birefringence relaxation over a broad range of annealing temperatures. A temperature dependent parameter is introduced in the stretched exponential function to account for the unrelaxed part of the frozen elastic strain. We also explored the ability to model the development of birefringence during fiber drawing in addition to birefringence relaxation using a pair of Jeffery models in parallel.

2. Experimental

2.1. Drawing apparatus

Our apparatus for continuously drawing fibers from cylindrical glass preforms is shown in Fig. 1. A cylindrical electric resistance heater softens the glass preforms. Thermocouples are embedded along the heater linear to monitor and control the temperature during fiber drawing. The heater power is supplied by a voltage transformer (manually controlled) and a proportional controller (DO-26, Omega). The glass preform is fed into the heater by a pair of feed roller controlled by a variable speed motor and a gear motor. The preform is heated by conduction, convection and predominantly radiation, to a temperature that softens glass. The winders, driven by a variable speed motor with PID control to insure a constant speed under variable load drawing conditions, draws the softened glass preform into a fiber. The air cooled fiber is collected after the winders.

Three millimetre diameter glass preforms (Corning 7740, 80.6% SiO_2, 13.0% B_2O_3, 4.0% Na_2O, 2.3% Al_2O_3, 0.1% miscellaneous by weight: ASTM annealing point 565°C) were drawn at various

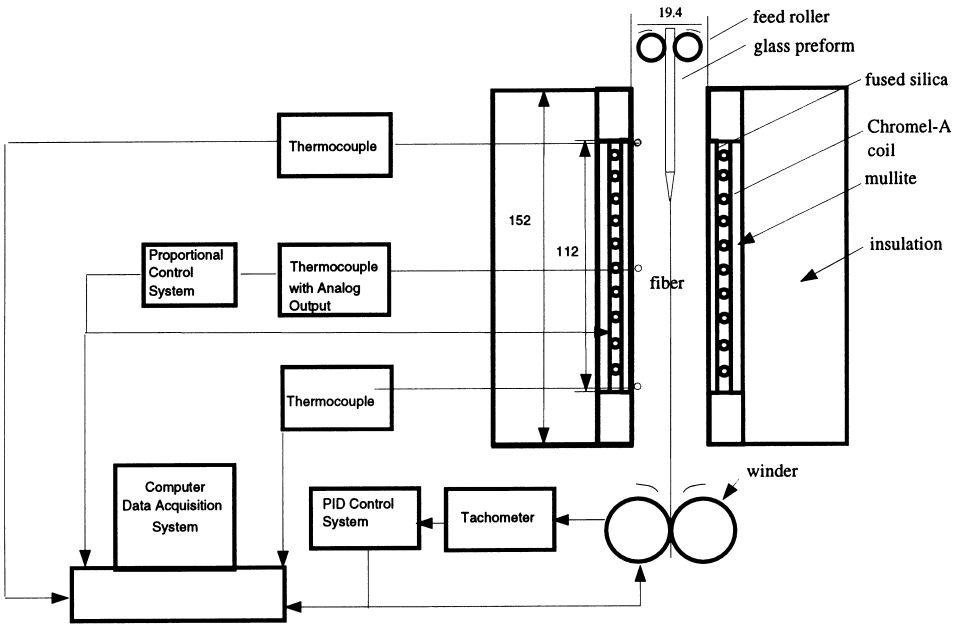

Fig. 1. Schematic of fiber drawing apparatus (all dimensions are in mm).

combinations of feed and winder speed and a range of drawing temperatures. This borosilicate glass was used instead of E-glass because it can easily be obtained in rod form.

The effect of drawing temperature, draw speed and draw ratio on the birefringence of drawn glass fibers has been examined. The drawing temperature T_m is defined as the maximum temperature along the spinline as measured by a thermocouple traversed down the centerline of the cylindrical heater when no fiber is being drawn. A typical temperature profile is illustrated in Fig. 2. In subsequent tests, the heater was controlled by T_m as estimated by a thermocouple placed just inside the fused silica at the approximate height of the maximum shown in Fig. 2. T_m was varied in the range of 1100 to 1215°C to study the effect of drawing temperature on birefringence. The location of the temperature maximum can be controlled be shields, variable winding spacing or convection suppression. For our uniform coil electric heater, the maximum occurs slightly higher than the heater midpoint due to natural convection.

The preforms were usually drawn at a feed speed of $v_f = 0.048$ mm s^{-1}, and drawing speed of $v_d = 212.0$ mm s^{-1} to produce 45 μm diameter fibers. Fiber diameter variations were less than 5%. A similar series of tests at $v_f = 0.027$ mm s^{-1} and $v_d = 119.0$ mm s^{-1} examined the effect of cooling rate on birefringence. A series of tests at $T_m = 1150$°C and 1215°C for $v_f = 0.048$ mm s^{-1} was conducted at various draw speeds to study the effect of draw ratio on birefringence. Fibers were carefully collected (without sizing) after the winder and stored in dessicators prior to preparation for birefringence measurements.

2.2. Birefringence measurement

It is difficult to measure the birefringence of a single glass fiber, since the retardation per unit thickness of glass is quite small (approximately 10^{-7} to 10^{-5}). Brückner [1] used an isotropic circular

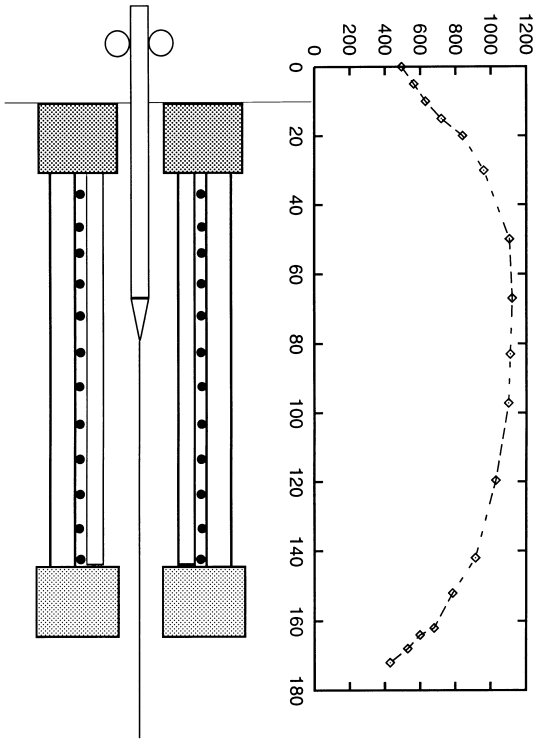

Fig. 2. The heater temperature (°C) along the spinline. The temperature measurements extend 10 mm above and 10 mm below the furnace.

quartz tube filled with many fibers to increase the retardation signal. The fibers in the tube were immersed in a refractive index matching liquid. We followed his approach, but used an optically isotropic square quartz tube to reduce scattering and refraction of a round tube. Fiber bundles were collected and pulled through the square quartz tube to increase the retardation signal. Up to five fiber tubes were stacked to further increase the retardation when birefringence becomes small (typically when the scaled birefringence becomes less than 0.1). The tube and fibers were then immersed in an index of refraction matching fluid to reduce light scattering from the fiber surfaces.

A polarizing microscope equipped with a tint plate (530 nm) first verified the existence of optical anisotropy in glass fibers. Quantitative fiber birefringence was measured with a polarizing microscope outfitted with a light intensity meter as illustrated in Fig. 3. The axial direction of the fiber sample is aligned at 45 degrees to the polarizer axis. The light intensity transmitted is measured and recorded by the intensity meter. The birefringence of the sample is calculated from

$$\Delta n = \kappa \frac{\lambda}{h\pi} \sin^{-1} \sqrt{\frac{I}{I_0}} \tag{12}$$

where Δn is the birefringence of the sample, κ a calibration coefficient of the polarizing microscope, λ the wavelength of the monochromatic light (589.6 nm), and h the effective thickness of the glass fibers in the tube. The effective thickness of the glass is computed from the weight, length and density of the

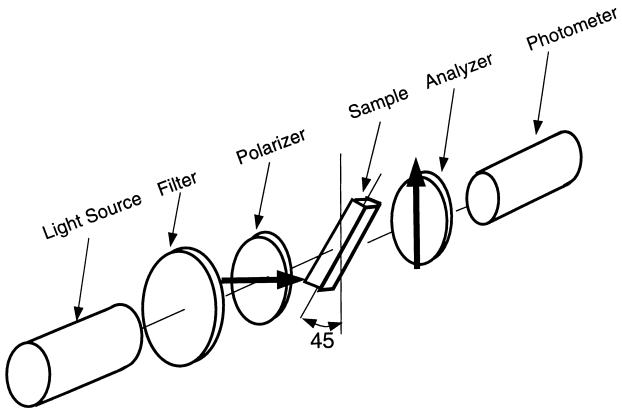

Fig. 3. Glass fiber birefringence measurement set-up.

fibers as $h = (w/\rho l)^{1/2}$. I_0 is the light intensity when the polarizer, analyzer and the fiber samples are all aligned in the same direction. I is the light intensity when the sample is rotated 45 degrees and the polarizer and the analyzer are crossed as shown in Fig. 3.

2.3. Post-processing

The birefringence relaxation of fibers was also studied by annealing the as-drawn fibers for various times and temperature. The samples were prepared as described above for birefringence measurement and annealed at constant temperature in a furnace maintained to within $\pm 2^{\circ}$C. Fibers were air quenched after annealing and held in a dessicator until tested. Two sets of fibers drawn at temperatures $T_m = 1150^{\circ}$C and 1215°C were used in the relaxation studies. The annealing temperatures ranged from 309°C to 511°C. The annealing time was recorded as the residence time in the furnace without regard to heat-up or cool-down times. The heat-up and cool-down times have been measured for some annealing processes. These results show that during heating and cooling the temperature approaches the specified temperatures exponentially with time constants in the range of 10 to 20 s. The effect of annealing furnace environment on birefringence relaxation was checked by varying relative humidity conditions for fibers annealed at 309°C for 180 min. Unlike Peng et al. [18] who studied moisture effects on structural relaxation for fibers under tension, the birefringence relaxation varied by less than 2% in our experiments.

3. Experimental results

Fig. 4 shows the variation of the as-drawn fiber birefringence with drawing temperature for different cooling rates. The different rates were achieved by varying feed and winder speeds at constant draw ratio as described in Section 2.1. Each datum represents the mean of three measurements. Error bars designate one-sigma variations. The birefringence of the as-drawn glass fibers decreases with increasing drawing temperature at constant draw ratio. The decrease in birefringence is moderate for drawing temperatures up to 1200°C; above 1200°C (near the working point, viscosity of 10^3 Pa s) the

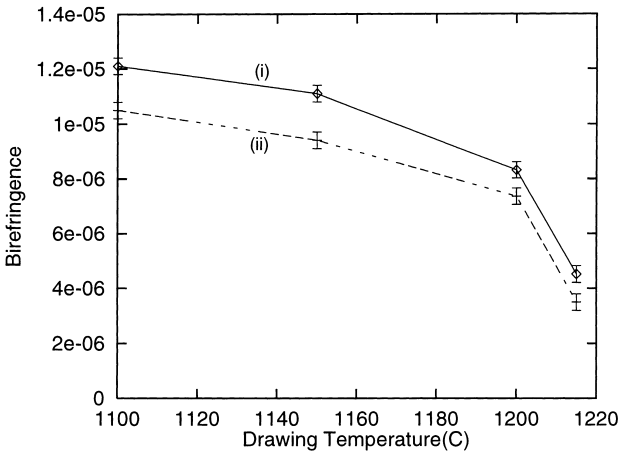

Fig. 4. The variation of the as-drawn glass fiber birefringence with temperature and cooling rate at constant draw ratio $v_d/v_f = 4410$. Cooling rate is increased by varying v_f and v_d to maintain a constant draw ratio. (i) High cooling rate, (ii) low cooling rate.

birefringence of the fibers drops significantly with draw temperature. This suggests that as the drawing temperature approaches the working point, the drawing tension and stress decrease quickly, causing the rapid reduction of the birefringence. The cooling rate during drawing was varied by proportionally changing the feed speed and winder speed to maintain a constant draw ratio. Fig. 4 results show that at constant draw temperature and draw ratio, the as-drawn birefringence increases with increasing cooling rate. This implies that a faster cooling rate is more effective at 'freezing' the anisotropic elastic strains developed during drawing deformation.

The effect of draw ratio on fiber birefringence was examined by varying the winder speed at constant feed speed shown in Fig. 5. The draw temperature was constant at $T_m = 1150°C$ and $T_m = 1215°C$ and

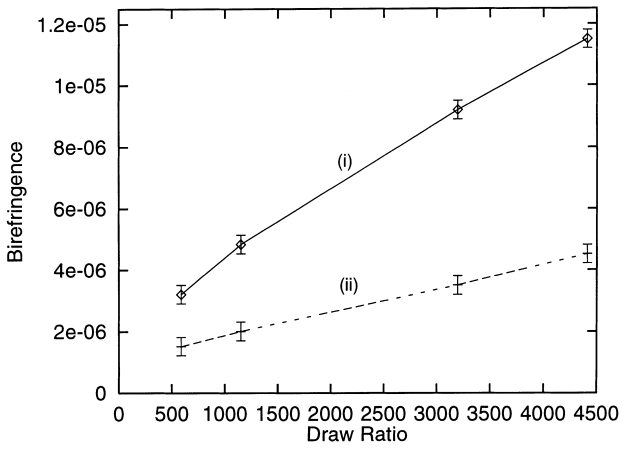

Fig. 5. The variation of as-drawn fiber birefringence with draw ratio at constant draw temperature (i) $T_m = 1150°C$, (ii) $T_m = 1215°C$

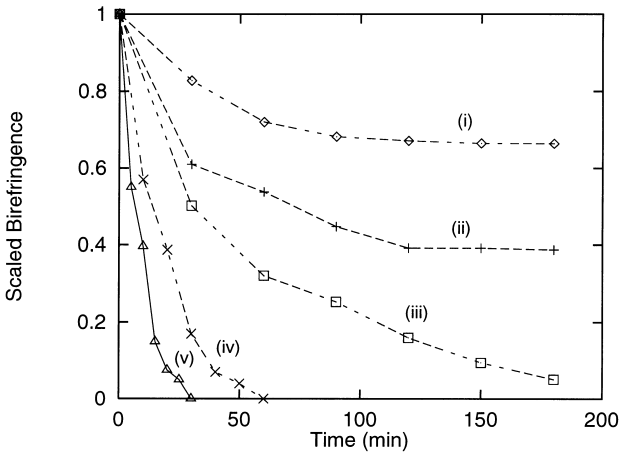

Fig. 6. The birefringence relaxation of glass fiber drawn at $T_m = 1215°C$ (draw ratio = 4410) for various annealing times and temperatures. Annealing temperatures (°C): (i) 309 (ii) 360 (iii) 387 (iv) 408 (v) 511.

the feed speed at $v_f = 0.048$ mm s^{-1}. Drawing speeds from 0.028 to 0.212 m s^{-1} resulted in draw ratios v_d/v_f of 587–4410, and corresponding fiber diameters of 120 μm–45 μm.

Fiber birefringence increases almost linearly with draw ratio in the range examined. At constant feed speed, the fiber diameter is inversely proportional to the square root of the drawing speed. Birefringence of glass fibers increases with increasing draw ratio or decreasing fiber diameter, and from momentum conservation, an increased drawing force results in increased draw ratio. Thus, these data confirm the expected trend of increasing birefringence with increasing tensile stresses or drawing forces. This would indicate that high draw ratios and low draw temperatures are preferential in developing birefringence and presumably stronger fibers. Unfortunately, the higher drawing forces are associated with fiber breaking during drawing and hence birefringence of as-drawn fibers significantly higher than that shown in Fig. 5 is hard to achieve.

3.1. Birefringence relaxation

Fig. 6 shows the birefringence relaxation of fibers drawn to $T_m = 1215°C$ and draw ratio of 4410 annealed at various times and temperatures. Fig. 6 includes results for all temperatures and annealing times up to 180 min. Fibers were annealed at 309°C for longer times and the results are reported in Fig. 7. At annealing temperatures of 408°C and above, birefringence relaxation is rapid and complete within 60 min annealing time. Fibers annealed at temperatures of 360°C and below appear to not fully relax as their birefringence asymptotes after 180 min. Fibers annealed at 309°C for longer times show no further relaxation after 24 h. Fiber annealed at 387°C show an intermediate behavior whereby relaxation is complete after an excess of 200 min.

Fig. 8 contains the relaxation results for fibers drawn at $T_m = 1150°C$ and a draw ratio of 4410. The relaxation behavior is similar to that shown in Fig. 6. Complete birefringence relaxation occurs quickly at annealing temperatures of 408°C and above; the birefringence does not fully relax at annealing temperatures below 360°C, and intermediate relaxation behavior is observed at 387°C.

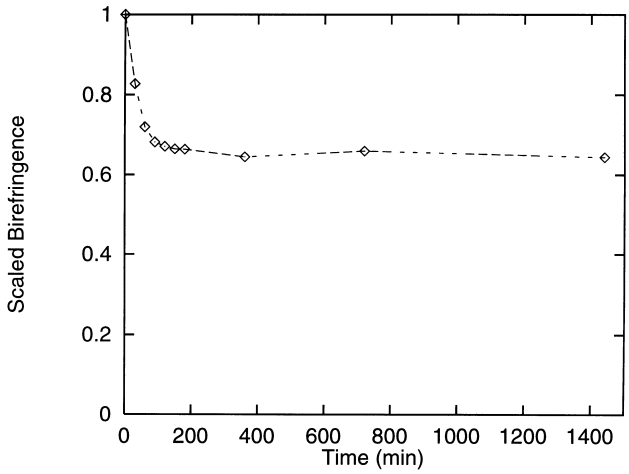

Fig. 7. Birefringence relaxation of glass fiber annealed at 309°C from Fig. 6 including longer times.

4. Relaxation modeling

Our experimental results show that oxide glass fiber birefringence relaxation in the glass transition range is qualitatively similar to that of the viscoelastic strain recovery of oxide glasses [19] in the glass transition temperature range. Glass structure and viscoelastic strain relaxation have been modeled using the stretched exponential (sometimes called the Kohlrausch–Williams–Watts or KWW function).

$$M(t) = \exp(-t/\tau)^b \tag{13}$$

where $M(t)$ is the relaxation function, τ the relaxation time and b a constant. Previous investigations have shown that b is around 0.5 for oxide glass stress relaxation or viscoelastic strain relaxation [20] in

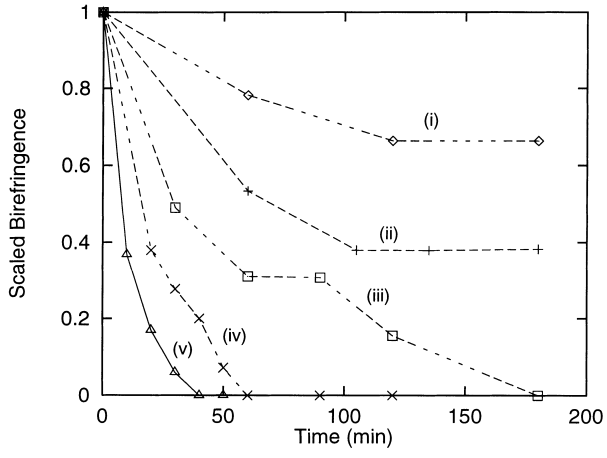

Fig. 8. The birefringence relaxation of glass fiber drawn at $T_m = 1150$°C (draw ratio = 4410) for various annealing times and temperatures. Annealing temperatures (°C): (i) 309 (ii) 360 (iii) 387 (iv) 408 (v) 511.

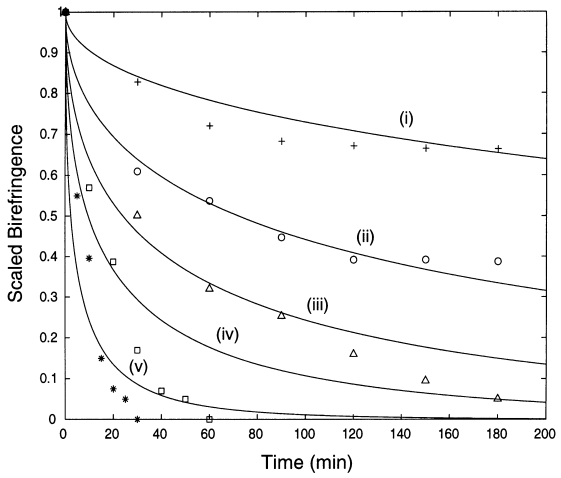

Fig. 9. Birefringence relaxation for fibers drawn at $T_m = 1215°C$. Data from Fig. 6. Lines are plotted using Eq. (13) with $b = 0.5$, and (i) $t = 309°C$, $\tau = 1000$ min; (ii) $T = 360°C$, $\tau = 150$ min; (ii) $T = 387°C$, $\tau = 50$ min; (iv) $T = 408°C$, $\tau = 20$ min; (v) $T = 511°C$, $\tau = 5$ min

the glass transition range. We explore the ability of the stretched exponential to simulate the glass fiber birefringence relaxation with the typical value of $b = 0.5$. The results for the scaled birefringence relaxation are shown in Fig. 9 using the relaxation times shown in the caption, chosen to best fit the data. Here, τ is assumed to be constant for the annealing time, so that the heating a cooling times for the fiber are neglected.

We can compare these relaxation times to those determined from viscosity and the elastic modulus as

$$\tau = \frac{\eta}{G}$$

where η is viscosity and G is the shear modulus of glass (assumed constant). As in [21], we find that the WLF or Arrhenius relationships are inadequate to describe the viscosity over a very large temperature range. Instead we use the Walther double exponential correlation

$$\eta = \eta_0 \exp[\exp(v_0 - v_1 \ln T)],$$

where η_0, v_0 and v_1 are constants for varying absolute temperature T. The correlation coefficients for Corning 7740 glass are $\eta_0 = 3.0$ Pa s, $v_0 = 18$ and $v_1 = 2.18$ ln K^{-1} from viscosity versus temperature data of Dormeus [22]. Using the Walther correlation results in a ratio of time constant of 10^{16} between $T = 309°C$ and $T = 511°C$ rather than the factor of 200 shown in Fig. 9. Clearly, the relaxation phenomenon is more complicated than what can be related by a single exponential relaxation time and the glass cannot be viewed as thermo-rheologically simple.

As Fig. 9 shows, at high annealing temperature ($T = 408°C$ and $511°C$), the stretched exponential with $b = 0.5$ does not fit the data well as the birefringence appears to relax to zero in finite time, while the simulation over-predicts the time of effectively complete relaxation by a factor of five. At low temperatures ($T = 309°C$) the birefringence does not fully relax for long times (24 h in Fig. 7). The exponential constant b may be varied for different relaxation temperatures without solving the problem.

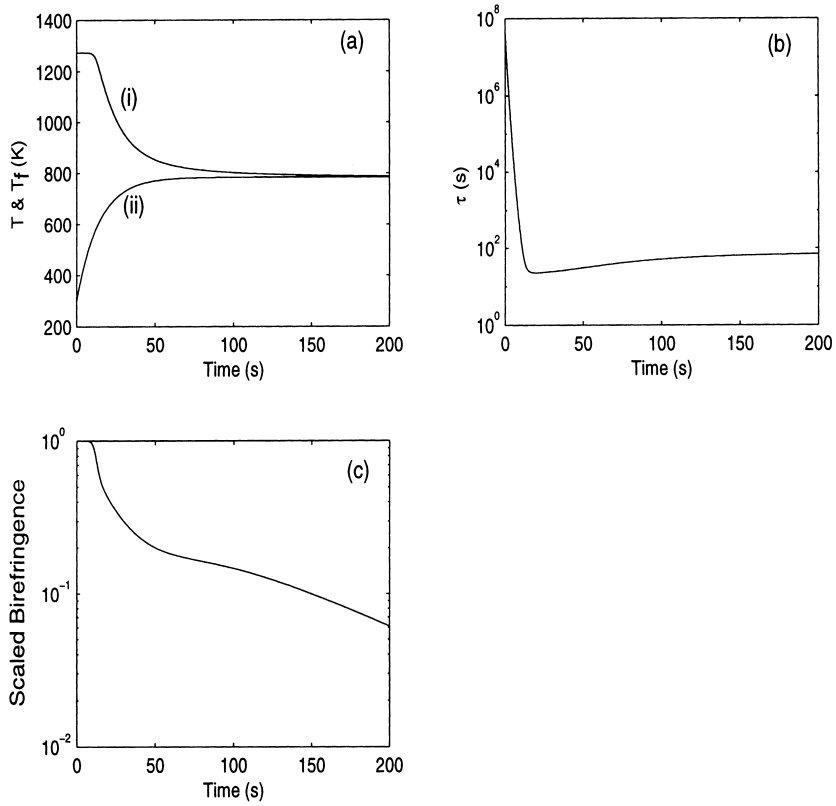

Fig. 10. Fictive temperature modeling of relaxation. (a) Temperature variation during annealing: (i) Fictive temperature T_f and (ii) fiber temperature T; (b) relaxation time evolution; and (c) birefringence relaxation.

Similarly, we model one relaxation case using T_f and Eqs. (3),(4),(6) and (9) with $b = 1$. For this case, we use the experimentally-determined time constant of 14 s for the temperature rise of the fibers at the beginning of the annealing process. We assume that $T_{f0} = 1273$ K to correspond with temperatures slightly lower than T_m, where most deformation will occur. The fictive and fiber temperatures are shown in Fig. 10 (a) for $\tau_0 = 10^{27}$ s, $a_1 = 5 \times 10^{-2}$/K, and $a_2 = 2.3 \times 10^{-2}$/K taken from Tool [8]. The evolution of the relaxation time τ and the scaled birefringence are then shown on Fig. 10((b) and (c)), respectively. As expected, this time-marching simulation shows that the scaled birefringence decays to zero, and now, the relaxation is slow at initial times. Clearly, this approach does not model relaxation either.

To capture the relaxation at low temperatures, the stretched exponential is modified by introducing a temperature dependent constant $C(T)$ such that

$$M(t) = [1 - c(T)]\exp(-t/\tau)^b + c(T) \tag{14}$$

Fig. 11 shows the simulation using Eq. (14) in a simplified form using $b = 1$. This modified relaxation function is capable of capturing all the relaxation data in Fig. 6.

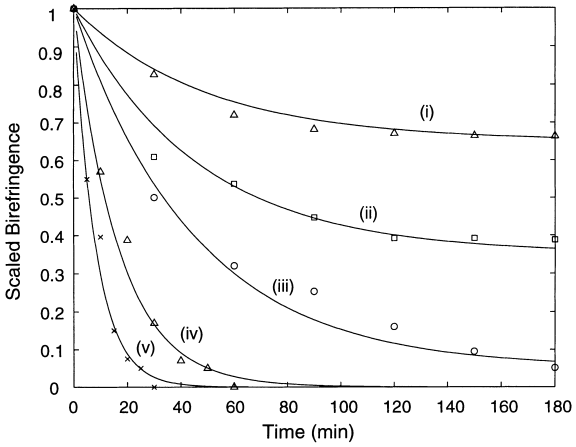

Fig. 11. Birefringence relaxation for fibers drawn at $T_m = 1215°C$. Data from Fig. 6. Lines are plotted using Eq. (14) with $b = 1$, and (i) $T = 309°C$, $\tau = 50$ min, $c(T) = 0.65$; (ii) $T = 360°C$, $\tau = 47$ min, $C(T) = 0.35$; (iii) $T = 387°C$, $\tau = 45$ min, $C(T) = 0.05$; (iv) $T = 408°C$, $\tau = 16.7$ min, $C(T) = 0.0$; (v) $T = 511°C$, $\tau = 8.24$ min, $C(T) = 0.0$.

5. Modeling birefringence with a two-component Jeffrey model

Eq. (14) shows that relaxation can be modeled using two exponential elements with at least one of them 'frozen' at low annealing temperatures (i.e. with very large relaxation times) to capture the incomplete relaxation. Eq. (14) offers limited physical interpretation and cannot simulate the development of birefringence during the drawing process. We explore a sample, two-component linearized Jeffrey element model shown in Fig. 12 to simulate both the drawing and relaxation processes. Here, either a tensile stress σ or elongation rate $\dot{\epsilon}$ can be applied.

In the parallel Jeffrey model, elements, μ_{12} and μ_{22} represent the large viscous deformation produced during the drawing process at high temperature. The two Kelvin elements represent the anisotropic elastic strain that is frozen during fiber cooling and relaxed during annealing. A minimum of two elements (two relaxation times) is required for incomplete relaxation. Since birefringence is a measure of anisotropic strain, we assume birefringence is proportional to the total strain in the two Kelvin elements. This anisotropic strain may partially or fully relax depending on the annealing temperature. The relaxation rate and extent of relaxation depend on the temperature dependent viscosities assigned to the viscous elements. The moduli of the spring elements are assumed constant.

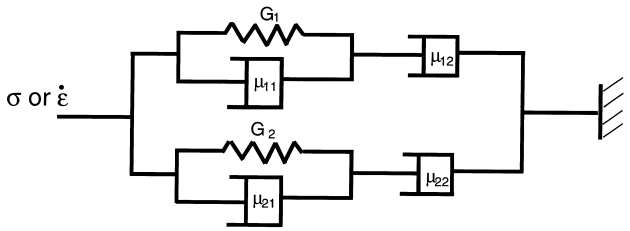

Fig. 12. Two Jeffrey element in parallel.

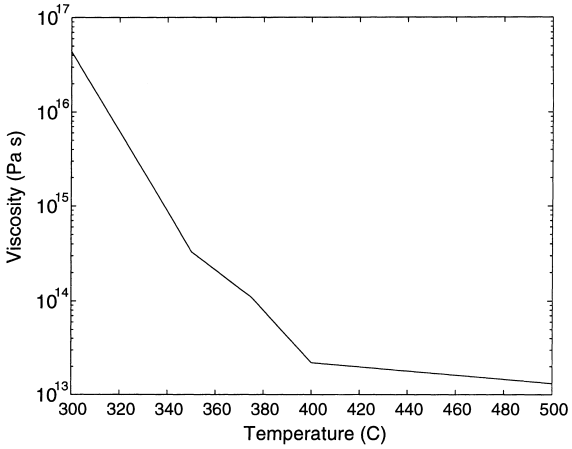

Fig. 13. μ_{11} versus annealing temperatures.

The linear, zero-dimensional model is used to simulate isothermal fiber drawing at a fixed drawing stress σ followed by instantaneous quenching to room temperature and frozen stresses. Drawing fibers at two temperatures to the same draw ratio requires less stress at higher drawing temperature. We stimulate drawing at $T_m = 1150°C$ using $\sigma = 10.0$ MPa, $G_1 = G_2 = 200$ MPa, $\mu_{11} = 10^8$ Pa s, $\mu_{21} = \mu_{12} = 10^6$ Pa s, $\mu_{22} = 10^4$ Pa s. By choosing the parameters for $T_m = 1215°C$ as $\sigma = 3.85$ MPa, $G_1 = G_2 = 200$ MPa, $\mu_{11} = 10^7$ Pa s, $\mu_{21} = 10^5$ Pa s, $\mu_{12} = 3.85 \times 10^5$ Pa s the ratio of as-drawn fiber birefringence is

$$\frac{\Delta n(T_m = 1150°C)}{\Delta n(T_m = 1215°C)} = 2.6 \tag{15}$$

in accordance with experiments of Fig. 5 at $\nu_d/\nu_f = 4410$. The draw rates are held constant by varying

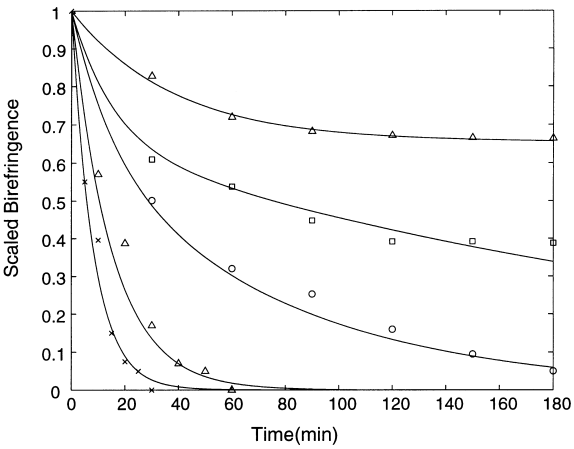

Fig. 14. Birefringence relaxation for fibers drawn at $T_m = 1215°C$. Data from Fig. 6. Lines are plotted using the two Jeffrey elements in parallel model.

the length of time that σ is applied. Thus we demonstrate that the two element Jeffrey model can qualitatively predict the development of birefringence during fiber drawing by arbitrarily varying (but in a physically appropriate way) these model coefficients.

We have also simulated birefringence relaxation at various annealing temperatures using the quenched system after fiber drawing (thermal expansion effects are neglected). The simplest temperature versus relaxation study using the Jeffrey model varies one parameter with temperature. We assume that the two elastic elements have a constant modulus of 24.4 GPa. Three of the viscous elements are assumed to have no temperature dependence in the annealing temperature range and their values are held as $\mu_{21} = 1.1 \times 10^{13}$ Pa s, $\mu_{12} = 2.2 \times 10^{11}$ Pa s, $\mu_{22} = 2.2 \times 10^{9}$ Pa s. The viscosity of the final viscous element μ_{11} varies with annealing temperature as shown in Fig. 13. This simple simulation of the parallel Jeffrey model is shown in Fig. 14 to model the birefringence relaxation of glass fibers over the entire range of annealing temperatures.

6. Discussion

Our results show that optical anisotropy develops during fiber drawing in glass fibers drawn from preforms. Optical anisotropy is the manifestation of the structural anisotropy which develops during the drawing process. In oxide glass, the structural and optical anisotropies are consequences of frozen anisotropic elastic strain by rapid cooling under the drawing load. The anisotropy of glass fibers has been studied using birefringence measurements for various drawing parameters. We show that the amount of the anisotropy is greatly affected by the draw temperature, the draw ratio and the draw rate.

Fiber birefringence increases with decreasing drawing temperature, increasing draw ratio, and increasing cooling rate. Increasing temperature drops the glass melt viscosity and the drawing force decreases and accordingly decreases the birefringence. Rapid cooling allows for less relaxation during drawing, thus the structure is quenched in an anisotropically strained state and the anisotropic structure exhibits birefringence. Increasing drawing speed increases draw ratio, this increased deformation also results in increased structural anisotropy and hence, birefringence.

We have observed glass fiber birefringence relaxation at temperatures well below the glass transition range in oxide glasses. At low temperatures, birefringence relaxation is observed, but relaxation is incomplete. This temperature dependent relaxation behavior suggests a broad spectrum of relaxation times. The generally used stretched exponential for delayed elastic strain and structural relaxation is not able to accurately simulate observed birefringence relaxation. A modified exponential model with incomplete relaxation simulates relaxation satisfactorily. A parallel Jeffrey model with temperature dependent coefficient simulates the glass fiber birefringence relaxation well not only for the high temperature annealing but also for low temperature annealing. The Jeffrey model enables simulation of the development of birefringence during fiber drawing as well as the relaxation process. The various elements in the Jeffrey model lend themselves to interpretation as viscous deformation elements or viscoelastic elements storing anisotropic strain at low temperature.

We are encouraged by these preliminary results and will continue to study steady fiber drawing using a one-dimensional nonlinear Jeffrey or canonical model and an accurate description of the temperature history during fiber drawing.

Acknowledgements

The financial support of the National Science Foundation (CMS #9414891) is gratefully acknowledged. We thank Dr. G.K. Gupta of Ford Motor Co. for preliminary model development.

References

[1] H. Stockhorst, R. Brückner, J. Non-Cryst. Solids 49 (1982) 471.
[2] H. Stockhorst, R. Brückner, J. Non-Cryst. Solids 86 (1985) 105.
[3] A.A. Griffith, Phil. Trans. Roy. Soc. A 221 (1920) 163.
[4] W.F. Thomas, Glass Tech. 12(2) (1971) 42.
[5] K.L. Loewenstein, J. Dowd, Glass Tech. 9(6) (1968) 164.
[6] X. Lu, Ph.D. Thesis, The University of Michigan, 1998.
[7] A.H. Cherin, An Introduction to Optical Fibers, McGraw-Hill, 1983.
[8] A.Q. Tool, J. Am. Ceram. Soc. 29 (1946) 240.
[9] H.N. Ritland, J. Am. Ceram. Soc. 39 (1956) 403.
[10] O.S. Narayanaswamy, J. Am. Ceram. Soc. 54(10) (1971) 401.
[11] G.W. Scherer, J. Am. Ceram. Soc. 67 (1984) 504.
[12] I.M. Hodge, J. Non-Cryst. Solids, 131–133 (1991) 435.
[13] I.M. Hodge, J. Res. Natl. Inst. Stand. Technol. 102 (1997) 195.
[14] J. Huang, P.K. Gupta, J. Non-Cryst. Solids 151 (1992) 175.
[15] H.S. Chen, C.R. Kurkjian, J. Am. Ceram. Soc. 66(9) (1983) 613.
[16] H.S. Chen, J. Non-Cryst. Solids 46 (1981) 289.
[17] A.R. Berens, I.M. Hodge, Macromolecules 15 (1982) 756.
[18] Yin-Lih Peng, M. Tomozawa, T.A. Blanchet, J. Non-Cryst. Solids 222 (1997) 376.
[19] D.H. Uhlmann, N.J. Kreidl (Eds.) Glass: Science and Technology, Academic Press, New York, 1986.
[20] G.W. Scherer, Relaxation in Glass and Composites, Wiley, New York, 1986.
[21] G.K. Gupta, W.W. Schultz, E.M. Arruda, X. Lu, Rheol. Acta 35 (1996) 584.
[22] R.H. Doremus, Glass Science, Wiley, New York 1973.